J. Am. Chem. Soc. **1993,** *115,* 5803–5812 5803

The Olefin Insertion Reaction into a Metal–Hydrogen Bond for Second-Row Transition-Metal Atoms, Including the Effects of Covalent Ligands

Per E. M. Siegbahn

Contribution from the Institute of Theoretical Physics, University of Stockholm, Vanadisvägen 9, S-11346 Stockholm, Sweden

Received November 19, 1992

Abstract: The olefin insertion into a transition metal–hydrogen bond has been studied for the entire sequence of second row transition metal atoms. Energies including correlation of all valence electrons have been obtained for geometry optimized structures of the reactants, of the π-bonded olefin complexes, of the transition states, and finally of the product metal–alkyl systems. To study the effects of covalent ligands the calculations were repeated with one and two additional hydride ligands. The main differences between the metals and also the main effects of the hydride ligands can be explained by a dominant role played by repulsion between nonbonding metal electrons and the olefin electrons. Clear consequences of this repulsion can be seen, for example, on the large barrier height increase between the niobium and molybdenum systems and also on the strikingly low barrier for insertion into the bond of the diatomic RhH. The systems to the left including the niobium complexes have low barriers because they can use empty 4d-orbitals to reduce the repulsion toward the olefin. The rhodium atom in RhH can reduce this repulsion by using the s^0-state for binding at the transition state. No relations can be noted between barrier heights and the bond strengths of the initial metal hydride or the strength of the π-bonded complexes.

I. Introduction

The olefin insertion into a transition-metal hydrogen bond, see Figure 1, is the key elementary step in some of the most important catalytical reactions. This is, for example, the case for olefin hydrogenation, olefin hydroformylation, and olefin isomerization. In many processes the same reaction in the reverse direction, that of β-hydrogen elimination, can instead be a significant step. From a fundamental and basic point of view, there are also many similarities between olefin insertion into a metal–hydrogen and into a metal–alkyl bond, which is the main elementary step in the technically very important Ziegler–Natta process for polymerization of olefins. The current status of theory on the olefin insertion into a metal–hydrogen bond, also called hydride migration to a coordinated olefin, has recently been reviewed by Koga and Morokuma.[1] The main orbital interactions involved in this reaction are by now well-characterized. Contributions to the present understanding have been given by Sakaki et al.[2] Fukui and Inagaki,[3] Thorn and Hoffmann,[4] and Koga et al.,[5] among others. One point of view[3,4] stresses the interaction between the highest occupied molecular orbital (HOMO), which has hydride contributions, and the lowest unoccupied molecular orbital (LUMO), which has mainly olefin π^* contributions. Another point of view[5] stresses the presence of efficient electron donation from the olefin π orbital to a σ^*_{MH} orbital and back-donation from the σ_{MH} orbital to the π^* orbital. These interactions facilitate the cleavage of the CC π and the MH σ bonds and the formation of the MC σ and CH σ bonds.

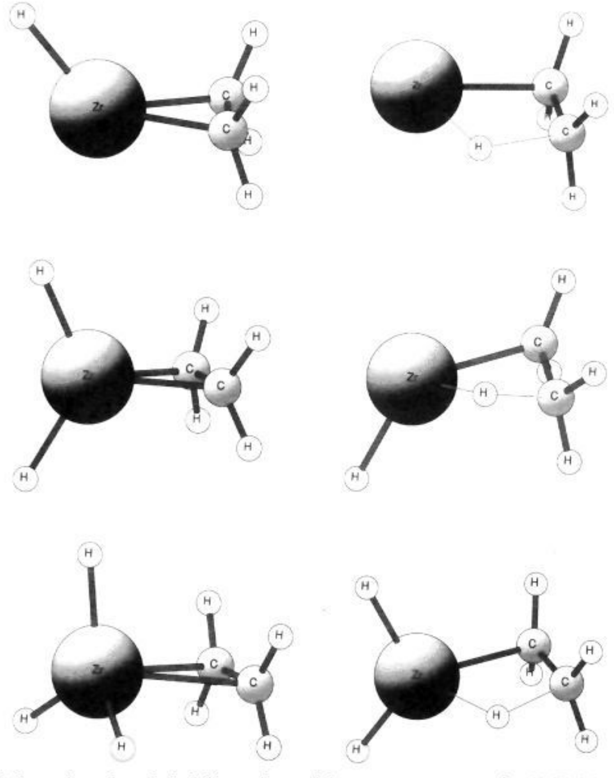

Figure 1. π-bonded olefin and transition-state structures for ZrH (a), ZrH_2 (b), and ZrH_3 (c).

If the main qualitative molecular orbital aspects of the olefin insertion reaction can be considered relatively well understood, the situation on the detailed energetics is less clear. Experimentally, an equilibrium between an olefin hydride and the corresponding alkyl species has been observed only rarely. An example involving a four-coordinated rhodium complex has been studied by Roe,[6] and another system involving a niobium complex was investigated by Doherty and Bercaw.[7] Theoretically, conclusions concerning the energetics have been based on only a few examples. Also, since these examples have involved coordinatively

---

(1) Koga, N.; Morokuma, K. In *Transition Metal Hydrides*; Dedieu, Ed.; VCH Publishers: New York, 1992; Chapter 6.

(2) Sakaki S; Kato, H.; Kanai, H.; Tarama, K. *Bull. Chem. Soc. Jpn.* **1975**, *48*, 813.

(3) Fukui; K.; Inagaki, S. *J. Am. Chem. Soc.* **1975**, *97*, 4445.

(4) Thorn, D. L.; Hoffmann, R. *J. Am. Chem. Soc.* **1978**, *100*, 2079.

(5) Koga, N.; Jin, S.-Q.; Morokuma, K. *J. Am. Chem. Soc.* **1988**, *110*, 3417.

(6) Roe, D. C. *J. Am. Chem. Soc.* **1983**, *105*, 7770.

(7) Doherty, N. M.; Bercaw, J. E. *J. Am. Chem. Soc.* **1985**, *107*, 2670.

0002-7863/93/1515-5803$04.00/0

saturated systems with a very large number of valence electrons, for quantum chemical standards, the accuracy of these calculations is not completely clear. The first more rigorous *ab initio* study of an olefin insertion into a metal–hydrogen bond was performed by Dedieu[8] for the Wilkinson catalyst. The study was made at the SCF level and with most of the geometrical parameters assumed. Quite reasonable results for the energetics of the reaction were obtained with an activation barrier of 13 kcal/mol and an exothermicity of 22 kcal/mol. More recently, Koga et al.[9] carried out a study on the same system but with all geometric parameters optimized using SCF energy gradient methods. They obtained an activation barrier of 18.6 kcal/mol and an exothermicity of 5.4 kcal/mol with energies calculated at the MP2 (Møller–Plesset second-order perturbation theory) level. A strong agostic interaction in the product was also noted. The energetic differences between the results of Dedieu and those of Koga et al. were found to be due to differences in the Rh–C distances used for the olefin complex. The Rh–C distance optimized at the SCF level is much longer by 0.4–0.5 Å than that assumed by Dedieu (see further discussion on this point below). Koga et al. also found another interesting effect in their study. Exchanging the chloride in the Wilkinson catalyst with a hydride changed the reaction energy in the first step of the insertion from being endothermic by 16.4 kcal/mol to being exothermic by 2 kcal/mol. The reason for this was found to be a weak chlorine trans effect which stabilized the metal–hydrogen bond involved in the hydride migration by 20 kcal/mol.

Even though the above-mentioned theoretical studies of the olefin insertion reaction have given important new insights into the mechanism of this reaction, it is clear that to get more detailed information and to gain further confidence in the energetics of this reaction more calculations are needed. The main purpose of the present study is to supply more energetic data on this reaction and also data obtained at a higher level of accuracy than the previous studies. It has been demonstrated in previous studies by Bauschlicher, Langhoff, and co-workers[10] and by our group[11] that a very useful approach to obtain a quantitative analysis of the energetics in reactions involving transition metals is to study an entire row of the periodic table. For example, this approach allows for a systematic evaluation of the importance of the positions of the various atomic states on the metal atom for the bonding. Also, the effects of a continuous increase of the ionization potential and an increase of the number of d-electrons of the metal can be investigated by going from left to right across the row in the periodic table. For the present study the second-row transition-metal series is selected. Most technical applications of the olefin insertion reaction and also most previous studies concern transition-metal complexes from this row. A major advantage of studying this row is that, based on previous experience, the geometry optimization can be performed at the SCF level with a high degree of confidence, in contrast to the case for complexes of the first row. Following the strategy of previous studies, the present study starts out with the reaction as simplified as possible. This means that in the first step no other ligands than the hydride and the olefin directly involved in the insertion process are present. The geometries and energies for the reactants (MH and C_2H_4), the product (MC_2H_5), the olefin π-complex, and the transition state for the reaction are obtained for every metal. In the energy calculations all valence electrons are correlated using reasonably large basis sets including f-functions on the metal (see Appendix for details). In the second step of this study the effects of ligands are investigated starting with one hydride and continuing with two hydride ligands. On the basis of the energetics of these 23 different reactions, it is then possible to approach a consistent description of the energetically most important electronic structure effects of the olefin insertion reaction, and this will be done below in the discussion and conclusion sections. One further comment is worth making at this stage. It will be seen below that ligands sometimes have substantial effects on the energetics of the reactions. However, the main electronic structure effects are the same with and without ligands. The tendency is that these effects will be exaggerated for the case without ligands. This is not only a disadvantage but it allows an easier identification and analysis of these effects to be made for the ligand-free case.

Table I. Product Geometries and Energies for the Olefin Addition Reaction: $MH + C_2H_4 + \Delta E \rightarrow MHC_2H_4$[a]

metal (M)	state	M–C	M–H_1	C–C	∠(H_1–MCC)	ΔE
Y	$^1A'$	2.28	2.07	1.56	53.3	–15.1
Zr	$^2A'$	2.20	1.95	1.52	49.8	–43.3
Nb	$^3A''$	2.28	1.87	1.46	56.0	–30.9
Mo	$^4A''$	2.28	1.78	1.47	67.9	–10.6
Tc	$^5A''$	2.33	1.84	1.44	0.0	–33.1
Ru[b]	$^2A'$					–21.4
Rh	$^1A'$	2.25	1.57	1.38	92.5	–27.5
Pd[c]	$^2A'$	2.42	1.58	1.39	0.0	–17.8

[4]a The energies are calculated relative to ground state metal hydrides and ethylene. H_1 is the hydrogen atom directly bonded to the metal atom and ∠(H_1–MCC) is the angle between the metal–hydrogen bond and the MCC plane. [b] Optimized geometry for $RhHC_2H_4$ used. [c] Geometry optimized at MP2 level.

Table II. Transition State Geometries and Barrier Heights for the Olefin Insertion Reaction: $MH + C_2H_4 + \Delta E \rightarrow MC_2H_5$[a]

metal (M)	state	M–C_2	M–C_1	M–H_1	C_2–H_1	C_1–C_2	ΔE
Y	^1A	2.88	2.63	2.04	1.81	1.39	–5.2
Zr	^2A	2.63	2.41	1.93	1.80	1.42	–11.7
Nb	^5A	2.61	2.39	1.81	1.73	1.40	–11.7
Mo	^6A	2.82	2.57	2.08	1.72	1.41	16.1
Tc	^5A	2.66	2.60	1.79	1.65	1.42	19.5
Ru	^2A	2.53	2.23	1.71	1.74	1.41	6.7
Rh	^1A	2.35	2.15	1.61	1.68	1.41	–12.8
Pd	^2A	2.42	2.29	1.76	1.65	1.42	6.9

[a] The energies are calculated relative to ground state metal hydrides and ethylene. C_1 is the carbon atom closest to the metal atom and H_1 is the hydrogen atom in the M–H bond which is inserted by the olefin.

Table III. Populations at the Transition State of the Olefin Insertion Reaction: $MH + C_2H_4 \rightarrow MC_2H_5$[a]

metal (M)	M(q)	4d	5s	5p	C_1(q)	C_2(q)	H_{2-5}(q)	H_1(q)
Y(^1A)	0.00	0.87	1.56	0.51	–0.23	–0.40	+0.18	–0.07
Zr(^2A)	0.00	2.19	1.32	0.44	–0.27	–0.39	+0.18	–0.03
Nb(^5A)	+0.05	3.93	0.74	0.24	–0.24	–0.38	+0.16	–0.06
Mo(^6A)	+0.05	4.69	0.92	0.30	–0.28	–0.36	+0.16	–0.05
Tc(^5A)	+0.05	5.97	0.64	0.30	–0.26	–0.37	+0.16	–0.04
Ru(^2A)	–0.02	7.57	0.27	0.13	–0.28	–0.28	+0.15	–0.01
Rh(^1A)	–0.10	8.59	0.31	0.14	–0.31	–0.25	+0.16	+0.05
Pd(^2A)	+0.09	9.41	0.21	0.22	–0.29	–0.35	+0.15	–0.07

[a] C_1 and H_1 are the carbon and hydrogen atoms closest to the metal atom. H_{2-5}(q) is the average charge of the hydrogens on the ethylene group.

II. Results and Discussion

The present study of 23 different examples of the olefin insertion into a metal–hydrogen bond represents a large amount of information. Only the main results of these calculations are collected in Tables I–X. For each reaction, the energies of the reactants, the products, the transition states, and the olefin π-complexes have been obtained for geometry optimized structures. The first set of reactions concerns the simplest possible model system, including only the hydride and olefin ligands directly

---

[8] Dedieu, A. *Inorg. Chem.* **1981**, *20*, 2803.

[9] (a) Koga, N.; Daniel, C.; Han, J.; Fu, X. Y.; Morokuma, K. *J. Am. Chem. Soc.* **1982**, *109*, 3455; (b) Daniel, C.; Koga, N.; Han, J.; Fu, X. Y.; Morokuma, K. *J. Am. Chem. Soc.* **1988**, *110*, 3773; (c) Koga, N.; Morokuma, K. In *The Challenge of d and f Electrons: Theory and Computation*; Edited by Salahub, D. R., Zerner, M. C.; Eds.; ACS Symp. Ser. 394; American Chemical Society: Washington, DC, 1980; p 77.

[10] Langhoff, S. R.; Pettersson, L. G. M.; Bauschlicher, C. W., Jr. *J. Chem. Phys.* **1987**, *86*, 268.

[11] Blomberg, M. R. A.; Siegbahn, P. E. M.; Svensson, M. *J. Am. Chem. Soc.* **1992**, *114*, 6095.

Table IV. Geometries and Energies for the Olefin Addition Reaction: $MH_2 + C_2H_4 + \Delta E \rightarrow MH_2C_2H_4$[a]

metal (M)	state	M–C	M–H$_1$	C–C	∠(H$_1$–M–H$_1$)	ΔE
Y	$^2B_2$	2.56	2.05	1.43	120.3	−25.1
Zr	$^1A_1$	2.19	1.92	1.51	121.6	−53.3
Nb	$^2A_2$	2.20	1.83	1.47	119.0	−43.3
Mo	$^3A_2$	2.20	1.83	1.47	119.0	−18.3
Tc	$^4A_2$	2.39	1.68	1.38	76.8	−13.4
Ru	$^3A_2$	2.55	1.68	1.36	67.6	−18.4
Rh[b]	$^2A_1$	2.10	1.89	1.44	22.6	−18.0
Pd[b]	$^1A_1$	2.13	1.89	1.43	22.6	−36.8

[a] The energies are calculated relative to ground state metal dihydrides and ethylene. H$_1$ is a hydrogen atom directly bonded to the metal atom. [b] Partly optimized at the MCPF level.

Table V. Transition State Geometries and Barrier Heights for the Olefin Insertion Reaction: $MH_2 + C_2H_4 + \Delta E \rightarrow MHC_2H_5$[a]

M	state	M–C$_1$	M–C$_2$	M–H$_1$	C$_2$–H$_1$	C$_1$–C$_2$	ΔE
Y	^2A	2.57	2.86	2.07	1.80	1.39	−6.9
Zr	^1A	2.29	2.40	1.89	1.57	1.48	−3.1
Nb	^2A	2.25	2.37	1.81	1.56	1.45	−10.7
Mo	^3A	2.22	2.32	1.74	1.59	1.45	4.3
Tc	^4A	2.29	2.44	1.74	1.58	1.42	2.4
Ru	^3A	2.31	2.49	1.69	1.60	1.41	−2.4
Rh	^2A	2.24	2.38	1.66	1.48	1.43	−0.9
Pd	^1A	2.20	2.38	1.65	1.46	1.42	−1.4

[a] The energies are calculated relative to ground state metal dihydrides and ethylene. C$_1$ is the carbon atom closest to the metal atom and H$_1$ is the hydrogen atom in the M–H bond which is inserted by the olefin.

Table VI. Populations at the Transition State of the Olefin Insertion Reaction: $MH_2 + C_2H_4 + \Delta E \rightarrow MHC_2H_5$[a]

metal (M)	M(q)	4d	5s	5p	C$_1$(q)	C$_2$(q)	H$_1$(q)	H$_2$(q)
Y(^2A)	+0.22	1.17	0.87	0.66	−0.22	−0.42	−0.10	−0.17
Zr(^1A)	+0.36	2.67	0.47	0.43	−0.30	−0.45	0.00	−0.20
Nb(^2A)	+0.20	3.63	0.75	0.37	−0.31	−0.41	+0.02	−0.13
Mo(^3A)	+0.14	4.96	0.56	0.29	−0.30	−0.37	+0.03	−0.09
Tc(^4A)	+0.14	5.77	0.67	0.36	−0.33	−0.35	+0.03	−0.15
Ru(^3A)	+0.05	7.00	0.52	0.38	−0.29	−0.35	+0.07	−0.13
Rh(^2A)	+0.03	8.12	0.48	0.37	−0.31	−0.31	+0.09	−0.11
Pd(^1A)	+0.01	9.12	0.50	0.30	−0.33	−0.29	+0.08	−0.16

[a] C$_1$ is the carbon atom closest to the metal atom, H$_1$ is the hydrogen atom in the M–H bond which is inserted by the olefin, and H$_2$ is a hydrogen atom directly bonded to the metal atom.

Table VII. Geometries and Energies for the Olefin Addition Reaction: $MH_3 + C_2H_4 + \Delta E \rightarrow MH_3C_2H_4$.

metal (M)	state	M–C	M–H$_1$	C–C	ΔE
Zr	$^2A''$	2.68	1.92	1.36	−18.6
Nb	$^1A'$	2.19	1.79	1.44	−40.3
Mo	$^2A''$	2.34	1.73	1.38	−15.6
Tc	$^1A'$	2.50	1.67	1.35	−10.1
Ru[b]	$^2A'$	2.42	1.68	1.36	−5.6

[a] The energies are calculated relative to ground state metal trihydrides and ethylene. H$_1$ is a hydrogen atom directly bonded to the metal atom. The M–C and M–H$_1$ distances are averaged distances. [b] Two hydrogen atoms appear as an H$_2$ molecule with an M–H$_1$ distance of 2.05 Å.

Table VIII. Transition State Geometries and Barrier Heights for the Olefin Insertion Reaction: $MH_3 + C_2H_4 + \Delta E \rightarrow MH_2C_2H_5$[a]

M	state	M–C$_1$	M–C$_2$	M–H$_1$	C$_2$–H$_1$	C$_1$–C$_2$	ΔE
Y	$^1A'$	2.55	2.86	2.09	1.79	1.40	−7.9
Zr	$^2A'$	2.43	2.67	1.93	1.77	1.40	−15.9
Nb	$^3A''$	2.41	2.69	1.89	1.78	1.40	−17.7
Mo	$^4A''$	2.39	2.63	1.80	1.67	1.40	−6.0
Tc	$^3A''$	2.28	2.43	1.72	1.56	1.43	−10.1
Ru	$^2A'$	2.20	2.33	1.68	1.61	1.43	−12.3
Rh	$^1A'$	2.16	2.36	1.62	1.65	1.41	−3.6

[a] The energies are calculated relative to ground state metal trihydrides and ethylene. C$_1$ is the carbon atom closest to the metal atom and H$_1$ is the hydrogen atom in the M–H bond which is inserted by the olefin.

Table IX. Populations at the Transition State of the Olefin Insertion Reaction: $MH_3 + C_2H_4 + \Delta E \rightarrow MH_2C_2H_5$[a]

metal (M)	M(q)	4d	5s	5p	C$_1$(q)	C$_2$(q)	H$_1$(q)	H$_2$(q)
Y($^1A'$)	+0.42	1.22	0.57	0.67	−0.20	−0.44	−0.13	−0.19
Zr($^2A'$)	+0.37	2.30	0.67	0.59	−0.26	−0.41	−0.06	−0.18
Nb($^3A''$)	+0.26	3.58	0.60	0.50	−0.25	−0.40	−0.05	−0.14
Mo($^4A''$)	+0.14	4.74	0.62	0.44	−0.28	−0.38	−0.01	−0.08
Tc($^3A''$)	+0.06	5.93	0.54	0.41	−0.34	−0.36	+0.04	−0.03
Ru($^2A'$)	−0.06	7.47	0.35	0.18	−0.30	−0.31	+0.05	+0.02
Rh($^1A'$)	−0.21	8.56	0.39	0.20	−0.31	−0.27	+0.08	+0.04

[a] C$_1$ is the carbon atom closest to the metal atom, H$_1$ is the hydrogen atom in the M–H bond which is inserted by the olefin, and H$_2$ is a hydrogen atom directly bonded to the metal atom.

Table X. Reaction Energies (kcal/mol) for the Olefin Insertion Reaction: $MH_x + C_2H_4 + \Delta E \rightarrow MH_{x-1}C_2H_5$[a]

M	$x = 1$	$x = 2$	$x = 3$
Y	−32.2	−30.5	−29.4
Zr	−36.4	−32.4	−33.9
Nb	−29.4	−33.3	−32.2
Mo	−29.1	−31.1	−30.1
Tc	−30.9	−28.3	−27.0
Ru	−26.1	−26.4	−27.0
Rh	−24.9	−24.8	−25.7
Pd	−27.0	−25.7	

[a] The energies are calculated relative to ground state metal hydrides and ethylene.

involved in the insertion process, see Figure 1a. These results are discussed and analyzed in the first subsection below. In the second subsection the effects of additional hydride ligands are discussed. This is done in two steps. First, by adding one hydride ligand as shown in Figure 1b and then by adding another hydride ligand as shown in Figure 1c. The main energetic trends of the present results are finally shown in Figures 2–5. The most interesting results are those for the transition states shown in Figure 2. It should be emphasized that these barrier heights are given with respect to the isolated metal hydrides and free ethylene. Experimentally, the reaction is normally viewed as a migratory insertion reaction starting from the olefin addition complexes. However, it turns out that the analysis of the trends in the barrier heights is much simpler starting from the free metal hydrides, and the results in Figure 2 are therefore the ones that will be discussed in the text below. For comparison, the olefin migratory insertion barriers are given in Figure 3. The overall reaction energy starting with free ethylene and the diatomic metal hydrides and ending with the metal alkyl insertion products are shown in Figure 4. The binding energies for π-bonding of ethylene to the reactant metal hydrides are shown in Figure 5.

(a) The Olefin Insertion without the Presence of Other Ligands. The main energetic results for the ligand free olefin insertion are best seen in Figures 2–5 and are denoted with $x = 1$. Starting with the overall reaction energies in Figure 4, these are quite stable with values between 25 and 35 kcal/mol for all metals. A notable trend toward smaller exothermicities going to the right in the row can also be seen. The exothermicity of the reaction is composed of two parts. There is first the energy gain for the formation of the new carbon–hydrogen bond, which also includes the breaking of the C–C π-bond. A good estimate of this energy gain can be obtained from the corresponding gas-phase reaction without the presence of the metal, i.e. the reaction between ethylene and a hydrogen atom to form the ethyl radical. The calculated value for this reaction energy is 42.2 kcal/mol. The second part of the reaction energy is the difference in bond strength between the metal–hydrogen bond broken and the metal–alkyl bond formed. Since the metal–hydrogen bond is stronger for all metals this contribution to the exothermicity is always negative. The largest difference in bond strengths are found for the atoms to the right, and this is thus the origin of the trend toward smaller exothermicities for these atoms. The reason for the increasing difference to the right in bond strengths between metal–hydrogen

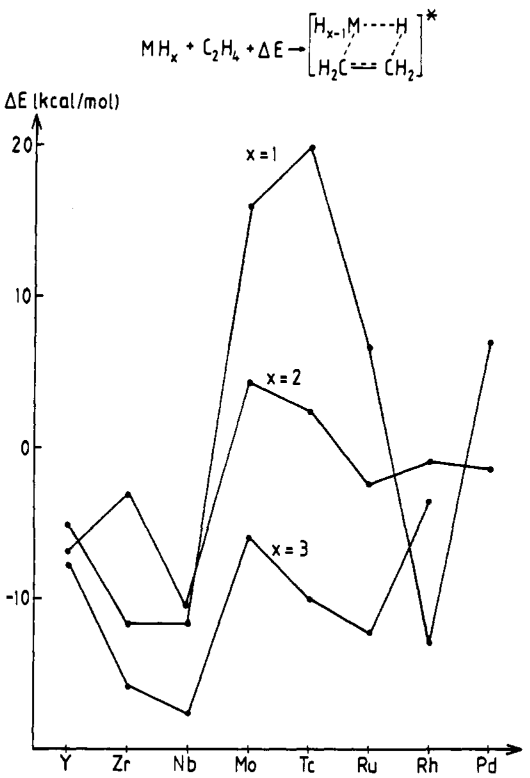

Figure 2. Transition-state energies for the olefin insertion reaction with MH_x, for $x = 1, 2, 3$. The energies are calculated relative to ground state MH_x systems and free ethylene.

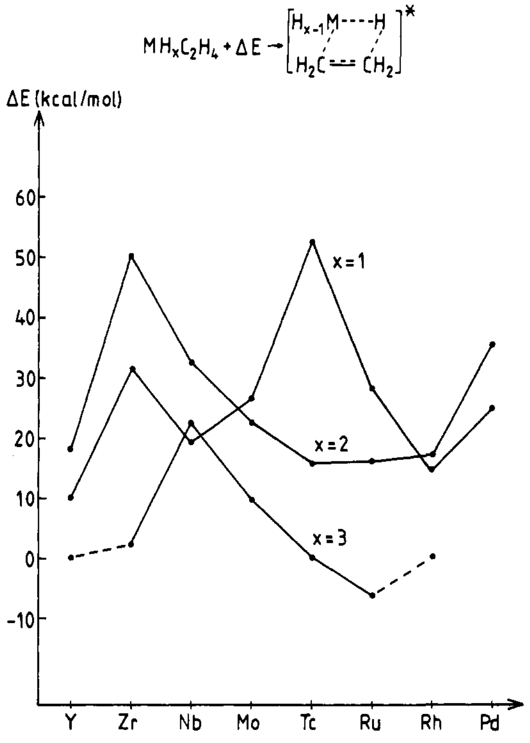

Figure 3. Transition-state energies for the olefin migration reaction in $MH_xC_2H_4$, for $x = 1, 2, 3$. The barriers are calculated relative to the ground state addition complexes of the MH_x systems and ethylene.

and metal–alkyl bonds is direct repulsion between the d-electrons and the ligand electrons, and this has been discussed recently with many more examples.[12] There are more electrons on the carbon atom than on the hydrogen atom, and the repulsion is therefore larger for the alkyl ligand and makes this bond weaker than the hydride bond. This repulsion is also larger the more d-electrons that are present, which makes the difference in bond strengths larger to the right. An interesting point noted in ref 12 is that the addition of electronegative ligands like hydrides makes the difference in metal–hydrogen and metal–alkyl bond strengths smaller. This occurs because the electronegative ligands remove some of the repulsive d-electrons from the metal. Direct ligand–ligand repulsion is of surprisingly small importance in this context. It should finally be noted that the relative constancy of the overall exothermicity, as shown in Figure 4, should not be interpreted as a stability of the individual metal–hydrogen and metal–alkyl bond strengths. As examples of the contrary, the Y–H bond strength is 68.0 kcal/mol whereas the Tc–H bond strength is only 42.3 kcal/mol. In spite of this large difference, the difference in the overall exothermicity of the yttrium reaction and the technetium reaction is only 1.3 kcal/mol.

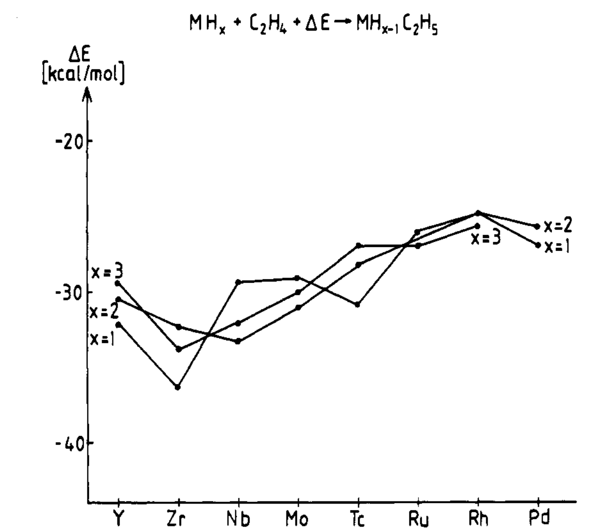

Figure 4. Overall reaction energies for the olefin insertion reaction with MH_x, for $x = 1, 2, 3$. The energies are calculated relative to ground state MH_x systems and free ethylene.

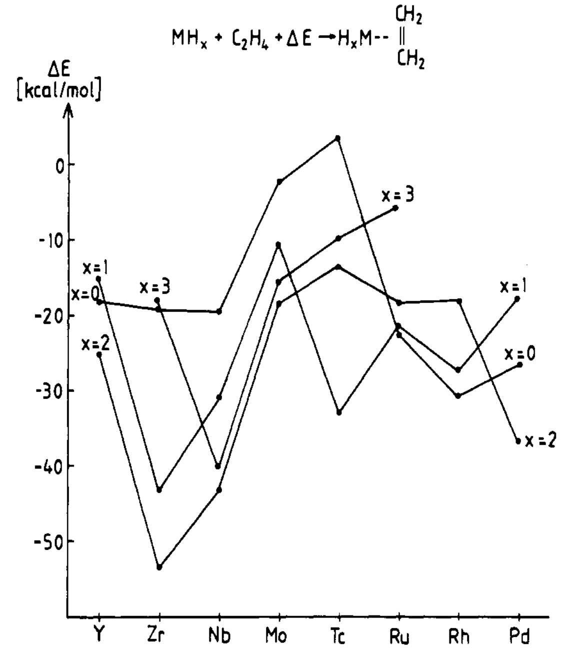

Figure 5. Binding energies for π-bonding of olefin to MH_x, for $x = 0, 1, 2, 3$. The energies are calculated relative to ground state MH_x systems and free ethylene. The energies for $x = 0$ are taken from ref 19.

The barrier heights for the ligand free olefin insertion, as shown for $x = 1$ in Figure 2, vary much more between the different metals than the overall reaction energies and are thus much more

---

[12] Siegbahn, P. E. M.; Blomberg, M. R. A.; Svensson, M. *J. Am. Chem. Soc.*, in press.

informative about the detailed energetics. The atoms to the left, yttrium, zirconium, and niobium, but also rhodium to the right have negative barrier heights between 5 and 13 kcal/mol. There are large barrier heights between 16 and 20 kcal/mol for molybdenum and technetium in the middle of the row, while ruthenium and palladium finally have barriers in between these extremes with 7 kcal/mol. It is of great importance to understand in detail two of these results in particular. First, why does rhodium, as the only atom to the right, have such a low barrier? In fact, the isolated sudden decrease of the barrier height for rhodium is so striking that the calculations were redone in order to confirm that no trivial error was present. Second, why does the barrier height increase so dramatically on going from niobium to molybdenum?

In order to understand the low barrier for rhodium, the main features of the electronic structure at the four-centered transition state have to be analyzed. The same main dissociation mechanism as noted in previous studies of the olefin insertion reaction[2-5] can be seen also on the wave functions of the systems studied here. There is one molecular orbital that is more critical than any of the others. This orbital is a linear combination of a metal d_{xy}-orbital, a hydride 1s-orbital, and the π- and π^*-orbitals on ethylene. This linear combination is such that there is positive, bonding overlap both between the metal and the hydrogen atom where the bond is being broken and between the metal and the carbon atom where a bond is being formed. At the same time there are only small contributions in this orbital from the carbon atom which is not directly bonded to the metal atom (the β-carbon). If the electronic structure at the transition state is compared to that of the free metal atom, the hydrogen atom, and the free olefin, the main interaction at the metal can be described as a formation of a single metal d-bond. This is one result that is important to keep in mind when the trends in Figure 2 are analyzed. The second important factor for the understanding of the low barrier for rhodium can be seen on the population analysis given in Table III. The point to note here is the high d-population and low sp-population for rhodium. Given the limitations of the population analysis, this is characteristic of an unusually clean d^9 state for rhodium. What is really important about this state is that it has a minimum number of the most repulsive electrons, the 5s-electrons, and to stress this importance we normally refer to this state as the s^0-state. This state was previously noted to be of key importance for the dissociation of C–H bonds[11,12] and also of C–C bonds,[13] and this is the reason the lowest barriers for these reactions are found to the right where this state is low-lying and of the right spin to be mixed into the wave function. The presence of the s^0-state at the transition state for the olefin insertion must mean that repulsive effects between the metal and the ligands are of great importance for the size of the barrier height for this reaction. With these two major facts made clear it is now possible to understand why the barrier is so much lower for rhodium than for both ruthenium and palladium.

The most illustrative example of the present analysis is given by the explanation for the large barrier height difference between rhodium and ruthenium of 19.5 kcal/mol. It should first be noted that the barrier heights given in Table II and Figure 2 are given with respect to the metal hydrides and the olefin. If the barrier heights are calculated with respect to the free metal atoms instead, the barrier height difference is even larger at 24.7 kcal/mol, since the RhH bond is 5.2 kcal/mol stronger than the RuH bond.[12,14] There are two main origins of the low barrier for rhodium. First, the promotion energy to reach the s^0-state for rhodium is small, only 7.8 kcal/mol. Secondly, there is no exchange energy lost when the d-bond is formed for rhodium since there are no other open shell orbitals present in the d^9-state of the atom. For ruthenium the necessary promotion energy is much higher, 25.1 kcal/mol and the exchange energy loss is 8.1 kcal/mol. The value obtained for the exchange energy loss is based on integrals given by Carter and Goddard.[15] The sum of the promotion and exchange energy differences leads to a predicted barrier height difference between rhodium and ruthenium of 25.4 kcal/mol, which is in almost perfect agreement with the actually computed difference of 24.7 kcal/mol. This is somewhat fortuitous, since other effects such as the number of d-electrons, the position of other atomic states on the metal, and detailed differences in the geometries also should give some contributions to the size of the barrier.

The barrier height difference between rhodium and palladium is somewhat more difficult to predict quantitatively, but the fact that there is a large difference is easy to rationalize. For palladium the s^0-state is the ground state, but since this state does not have any open d-orbitals it cannot form the necessary bond at the transition state. The cost for the promotion to the d^9s-state is as high as 21.9 kcal/mol. Another problem with the d^9s-state is that the s-electron in this state introduces a repulsion toward the olefin. As seen in the population analysis in Table III, the choice made is to stay to a large extent in the s^0-state at the price of a significantly weaker Pd–H bond. This is thus a good illustration of the importance of ligand repulsion at the transition state. Considering the combination of a large promotion energy to a bonding state, some loss of exchange energy (about 4 kcal/mol), and a large loss of metal–hydrogen bonding for PdH, a large difference in barrier height of 19.7 kcal/mol between palladium and rhodium is what should be expected.

The explanation for the large increase in barrier height between niobium and molybdenum is related to, but still different from, the origin of the sudden decrease in barrier height for rhodium, described above. The similarity is that the barrier height increase for molybdenum is due to metal–ligand repulsion effects. One difference is that the s^0-state is not involved for the atoms to the left since it has the wrong spin to be mixed into the wave function for these atoms. The fist intuitive explanation for the increase in barrier height for molybdenum is that this is connnected with the fact that this is the first atom, going from the left, which does not have any empty d-orbitals. A similar decrease in binding energy at molybdenum has thus been seen previously for the transition-metal halides,[14] for the oxides,[16] and also for the products of the O–H insertion reaction of water[17] and for the N–H insertion in ammonia[18] In all these cases the explanation for the larger stability of the niobium complex than of the molybdenum complex is direct electron donation to an empty d-orbital for the niobium complex. Therefore, it is interesting to note that any donation of this type cannot be seen on the wave function for the olefin insertion reaction. Instead, a quite marked difference occurs in the metal orbital hybridization at the transition states for niobium and molybdenum. As already mentioned, the repulsion between the metal electrons, in particular for the metal s-electrons, and those of the olefin represents a key factor for the size of the barrier of the reaction. A large part of this repulsion can be removed for niobium by hybridizing the 5s-orbital with the empty and the occupied 4d-orbitals. For niobium, the s-electrons are therefore involved in two hybrids with the d-orbitals which both point away from the olefin. For molybdenum there is no gain in the hybridization between the s- and the d-orbitals since they are all singly occupied and the wave function is energy invariant to rotations among equally occupied orbitals. At the transition state for the molybdenum reaction, the 5s-orbital therefore does not contain any contributions from the 4d-orbitals but mixes to some extent with the 5p-orbitals, which still makes the interaction with the olefin quite repulsive. This is the main

---

(13) Siegbahn, P. E. M.; Blomberg, M. R. A. *J. Am. Chem. Soc.*, in press.

(14) Siegbahn, P. E. M. *Theor. Chim. Acta*, in press.

(15) Carter, E. A.; Goddard, W. A., III *J. Phys. Chem.* **1988**, *92*, 5679.

(16) Siegbahn, P. E. M. *Chem. Phys. Lett.* **1993**, *201*, 15.

(17) Siegbahn, P. E. M.; Blomberg, M. R. A.; Svensson, M. *J. Phys. Chem.* **1993**, *97*, 2564.

(18) Siegbahn, P. E. M.; Blomberg, M. R. A.; Svensson, M. *Inorg. Chem.*, submitted for publication.

origin of the high barriers for both molybdenum and technetium. A large loss of exchange energy for these systems also plays a role but cannot, for example, explain the difference between niobium and technetium since these systems have the same spin.

Following the analysis above it is thus straightforward to understand even the seemingly irregular shape of the barrier height curve for $x = 1$ in Figure 2 in almost quantitative detail. It is interesting and important to note that some simple, intuitive explanations are in strong disagreement with the present results. One such explanation would be that the ease of olefin insertion should be roughly inversely proportional to the strength of the metal–hydrogen bond that is being inserted. It might be argued that TcH, which has by far the weakest metal–hydrogen bond of all the diatomic metal hydrides at 42.3 kcal/mol, should have the lowest barrier for olefin insertion. Actually, by coincidence, the exactly opposite occurs, namely that TcH has the highest barrier of all the hydrides in the second row at 19.5 kcal/mol. As seen on the exothermicities in Figure 5 and in Table X, this is *not* connected with a low overall reaction exothermicity for TcH, which has a value close to the average of the other metals. A general correlation indicating that the *strongest* metal–hydrogen bonds should be easiest to insert, which would be a very surprising result, does not occur either. For example, ZrH has one of the weakest bonds at 56.0 kcal/mol but almost the lowest insertion barrier at −11.7 kcal/mol. Another correlation which is tempting to search for is a correlation between the olefin bond strength and the barrier height for the insertion. Any such relation is not supported by the present results either. MoH has the weakest metal–olefin bond at 10.6 kcal/mol and the next to the highest barrier for insertion at 16.1 kcal/mol. On the other hand, the second weakest metal–olefin bond is found for YH at 15.1 kcal/mol, which has one of the lowest barriers at −5.2 kcal/mol. The highest barrier is found for TcH which has one of the strongest metal–olefin bonds at 33.1 kcal/mol, etc.

As already indicated above, the metal–olefin bond strengths show no direct relation with either the barrier heights or the final reaction exothermicities. These bond strengths are still of substantial interest for the olefin insertion, in particular since these complexes can represent the lowest point on the potential energy surface. This is definitely the case for zirconium, and probably also for niobium, technetium, and rhodium. The details of the variations of the metal–olefin bond strengths can be understood by considering promotion and exchange loss effects, but we will not go through this full analysis for every complex here. Only some illustrative examples will be discussed. The olefin binding energy for ZrH is 24.3 kcal/mol stronger than the one for the Zr atom, which has a value of 19.0 kcal/mol at the same level of accuracy.[19] This difference can be explained to a large extent by differences in promotion and exchange effects which amount to 18.9 kcal/mol.[12] The promotion energy difference is 12.0 kcal/mol, and the exchange energy difference is 6.9 kcal/mol. For the atoms in the middle of the row, the olefin binding energies are larger for the hydrides than for the naked atoms. Part of this can be explained by a smaller exchange loss for the hydrides, which have lower spins than the atoms, but a reduction of the direct repulsion is also important. The hydrogen atom in the diatomic hydride removes some of the repulsive electrons from the metal and therefore increases the binding energy to the olefin. For the atoms to the right there is a computational problem which deserves some attention. The π-bonded olefin complexes for these atoms are the only ones of the present structures where the geometry optimization is problematic. The reason for this problem is a combination of the fact that the binding at the SCF level is very weak and that the donation–back-donation bond dissociates correctly at the SCF level. Therefore, much too long metal–carbon bond distances are obtained at the SCF level. This bond distance therefore needs to be optimized at a correlated level or it can often to a good approximation be taken from some nearby olefin complex for which this problem does not occur. It is interesting to note in this context that the rhodium–carbon bond distance of 2.15 Å assumed by Dedieu[8] for the Wilkinson catalyst is rather close to the one obtained in the present study based on several different methods of determining this bond distance. Therefore, the opposite conclusion to the one drawn by Koga et al.[9] (see the discussion in the introduction) about this bond distance is drawn here, namely that the bond distance optimized at the SCF level is not reliable.

(b) Covalent Ligand Effects on the Olefin Insertion. In the previous subsection it has been shown that for the simplest possible model of the olefin insertion reaction, it is possible to understand every effect and to break down the energies involved in these effects in terms of detailed interactions. Since the final goal is to understand more realistic systems, which can actually be observed under normal laboratory conditions, the next step in this analysis is to study the effects of adding ligands to the metal. A general investigation of ligand effects on the olefin insertion reaction would clearly carry too far, and the present investigation is therefore restricted to covalent ligands. Covalent ligands here mean ligands that change the oxidation state of the metal. The reason for the choice to start an investigation of ligand effects with covalent ligands is that this type of ligand is expected to have the largest influence on the reaction energetics. To model covalent ligands, hydrogen atoms are chosen here, since they are the simplest models of this kind, and since they are still representative of many of the effects that can appear when ligands are added.

The discussion of ligand effects will start directly with the transition states, since these are the most interesting results. A typical transition-state structure for MH_2 and C_2H_4 is shown in Figure 1b and one for MH_3 and C_2H_4 is shown in Figure 1c. The corresponding π-bonded olefin structures are given in the same figure. The transition-state barriers and detailed geometries are given for MH_2 in Table V and for MH_3 in Table VIII while the main results of the population analysis are given in Tables VI and IX, respectively. The main energetic results for the transition states are as before best seen in Figure 2.

The most striking effect of adding covalent ligands is a significant reduction of the size and the variation of the barrier heights. This effect is clearly seen already for the MH_2 reactions ($x = 2$, in Figure 2) with one additional ligand and is further emphasized for the MH_3 reactions ($x = 3$) with two ligands. For the MH_2 reactions the largest barrier height occurs for molybdenum with 4.3 kcal/mol which is much smaller than the largest barrier height for the MH reactions where technetium has a barrier of 19.5 kcal/mol. For the MH_3 reactions the largest barrier height is in fact negative at −3.6 kcal/mol and occurs for rhodium. The difference between the largest and smallest barrier height is 32.3 kcal/mol for the MH reaction and 15.0 kcal/mol for the MH_2 reaction, and for the MH_3 reaction it is only slightly smaller at 14.1 kcal/mol.

The fact that the results for the different metals have become more similar when covalent ligands are added does not mean that the effects discussed in subsection a are not present and no longer of interest. The main effect noted was the significant contribution to the differences of the barrier heights that come from direct repulsive effects between the olefin and the nonbonding electrons on the metal. The effect of this interaction could be seen on mainly two positions in Figure 2. First, there is a very sharp increase in barrier height between niobium and molybdenum. It is interesting to note that in this region all three curves show a similar behavior. The sd-hybridization effect which makes use of the empty 4d-orbital on niobium is thus still present but somewhat reduced when ligands are added. The second position in Figure 2 where the metal repulsion effects could be clearly seen for $x = 1$ was for rhodium where there is a very deep minimum

---

(19) Blomberg, M. R. A.; Siegbahn, P. E. M.; Svensson, M. *J. Phys. Chem.* **1992**, *96*, 9794.

due to bonding with the non-repulsive $4d^9$-state. Since this state can only form one covalent bond, this minimum has disappeared in the figure for $x = 2$ and 3, where the metal is required to form two and three covalent bonds, respectively. This means that the state involved for rhodium will be the $4d^85s^1$-state instead, which is not less repulsive than the states involved for any of the other metals to the right. For $x = 2$ and 3, the importance of the repulsion between the metal electrons and the ligand electrons for the barrier height is perhaps best seen from the fact that the barriers are lower for the atoms to the left which have fewer repulsive 4d-electrons.

The dominating role of repulsion involving nonbonding metal electrons for the size of the barriers is also the best explanation for the fact that the barriers decrease as covalent ligands are added. The hydride ligands will simply remove (or redistribute, see below) some of the repulsive electrons on the metal and thereby reduce the repulsion to the olefin and make the barriers smaller. This conclusion is in some sense trivial if the conventional notion of the oxidation state of a metal is adapted. For example, an M(II) metal which has two covalent bonds is then considered to have a charge of +2, and it should therefore have fewer electrons and thus be much less repulsive toward ligands than an M(I) metal. However, an important point to note in this context is that the changes of the charge on the metal as more covalent ligands are added are much more subtle than the oxidation state would indicate. In fact, for the metals to the right the metal is almost neutral for all three different reactions with $x = 1, 2, 3$. Therefore, a modeling of covalent ligand effects by increasing the charge on the metal by one unit for every covalent ligand would give a quite exaggerated, not to say the wrong, picture of the true situation. A different and in some situations better description of the effect of the covalent ligand is that it gives the metal a possibility to redistribute its electrons. This redistribution of electrons will be such that the energy is minimized and thereby also the repulsion to the ligands. By having a picture of the covalent ligand effect of this type it is also easier to accept actual differences between, for example, hydride and chloride ligands. An intuitive expectation of what would happen if a hydride is exchanged with a chloride ligand for the olefin insertion is that this would always reduce the size of the barrier since the chloride should remove more electrons from the metal than the hydride does. Based on the picture that the main effect of the ligand is to redistribute the electrons on the metal, the conclusion about the ligand effects is less obvious. A preliminary comparative study of hydride and chloride ligand effects on the oxidative addition of H_2 and CH_4 indicates that the differences between these ligands can vary in a surprising manner,[20] and the effects on the olefin insertion of having chloride ligands are therefore too early to predict at this stage.

As noted in Figure 2 for $x = 2$, the barrier heights for the metals from molybdenum to rhodium are almost constant. This fact is fairly easy to rationalize. At the transition state two bonds are formed. One of these bonds is the d-bond described in subsection **a**, and the other bond is the bond to the non-participating hydride ligand. The atomic state of the metal that forms these two bonds is the s^1-state for all of the metals from molybdenum to palladium. This is the same state as forms the two bonds in the dihydrides of these metals, and since the barrier heights for the $x = 2$ reaction in Figure 2 are calculated with respect to the dihydrides, all promotion and exchange effects will cancel for the barrier height. This is different from the $x = 1$ reaction, where the single bond at the transition state is a d-bond, whereas the bond in MH is an s-bond. Different atomic states are therefore involved for the reactants and at the transition state, which leads to the large variation of the barrier heights observed in this case.

For the MH_2 and MH_3 reaction curves in Figure 2 another effect of interest can also be noted. For most of the covalently saturated systems (the singlet systems) there is a marked increase of the barrier height compared to the metals closest to these systems. For the ZrH_2 system, which is a singlet, the barrier is 3.8 kcal/mol higher than for YH_2 and 7.6 kcal/mol higher than for NbH_2. For YH_3, which is a saturated singlet, the barrier is 8.0 kcal/mol higher than for ZrH_3 and for RhH_3 the barrier is 8.7 kcal/mol higher than for RuH_3. The only exception to this behavior is PdH_2 which is saturated but still has a barrier very similar to that of the nearby RhH_2. The origin of these results is probably that for the saturated systems all hybrids are being used for bonding and there are certain directions of these bonds which are more optimal than others. For the free metal hydrides the geometry is free to adapt to the available hybridization. This is not the case at the transition state, where for example the hydride ligands must not interfere with bond-breaking and bond-formation or come to close to the olefin.

An interesting geometric effect can be noted on the transition states for the MH_2 reactions. The geometry optimizations for these systems were performed without any symmetry constraints, since the additional ligand hydride is expected to point out of the plane defined by the transition-state structure found for $x = 1$. This turns out to be the case for the MH_2 transition states for the metal atoms to the left but not for those to the right which adapt planar geometries (apart from the hydrogens on the olefin). This result was initially considered quite surprising since the corresponding free MH_3 systems behave in exactly the opposite way with planar geometries to the left and nonplanar to the right.[12] The origin of the differences in the free MH_3 structures is differences in hybridization. The metal atoms to the right form more covalent M–H bonds based on sd-hybridization on the metal, and this type of hybridization will favor nonplanar structures of the free MH_3. This is easy to understand by considering the bonding between MH_2 and a hydrogen atom (see further details in ref 21). The metal atoms to the left, on the other hand, will form more ionic M–H bonds based on sp-hybridization, and it is equally easy to see that this will lead to planar MH_3 systems. It is interesting to note that the same explanation as used for the free MH_3 systems can be used to explain the opposite behavior for the transition states for the MH_2 olefin insertion reactions. It was pointed out in subsection **a** for the $x = 1$ reactions that the origin of the marked increase in barrier heights between niobium and molybdenum is due to hybridization effects. For niobium the nonbonding s- and d-electrons can be placed in sd-hybrids that point away from the olefin, and this will reduce the repulsion and lower the barrier heights in an effective way. This sd-hybridization requires the use of empty 4d-orbitals, and it can therefore not be used for molybdenum which lacks empty 4d-orbitals. A mixing of orbitals with equal occupation will not change the energy and it will therefore not reduce the repulsion. The main effect on the olefin insertion reaction of the addition of the hydride ligands for the atoms to the right is to remove some repulsive electrons from the metal olefin region, and this type of interaction makes use of sp-hybridization. The situation for the olefin insertion, with sd-hybridization to the left and sp-hybridization to the right, is thus exactly opposite to the one for the MH_3 systems. However, the explanation for the planarity and nonplanarity is the same for the two cases with sd-hybridization favoring nonplanar geometries and sp-polarization favoring planar geometries.

A few words should finally be said about the π-bonded olefin complexes. As already noted in subsection **a**, there is no direct connection between the barrier heights of the olefin insertion and the metal–olefin bond strengths, but the ligand effects on the latter are still of some general interest. The metal–olefin bond strengths vary strongly between the metals and also with the number of hydride ligands. These variations, as shown in Figure 5, may appear somewhat random, but most of them are in fact

---

(20) Siegbahn, P. E. M.; Blomberg, M. R. A., to be submitted for publication.

(21) Blomberg, M. R. A.; Siegbahn, P. E. M.; Svensson, M. *New J. Chem.* **1991**, *15*, 727.

rather easy to understand. Some of the more general trends will be discussed here starting with the results for zirconium. When the zirconium atom binds an olefin, the atom is promoted to the s^1-state since the ground s^2-state is too repulsive. There is also a loss of exchange energy when the bonds are formed, which together with the promotion energy of 14.4 kcal/mol leads to a rather weak metal–olefin bond of 19.0 kcal/mol. For ZrH the metal–olefin bond is much stronger at 43.3 kcal/mol. Most of the increase in the bond strength can be explained by a reduction in promotion and exchange loss energies, as discussed in subsection **a**. For ZrH_2 there is no promotion energy involved when forming the π-bond to the olefin, and the exchange loss is smaller than for ZrH which leads to a still larger binding energy of 53.3 kcal/mol. In the metal–olefin complex of ZrH_2 the bonding is saturated with all the four zirconium valence electrons being occupied in bonding, two of them in the metallacyclic bonds to the olefin. When another hydrogen is added forming the olefin complex for ZrH_3, it is only possible to form one bond to the olefin and the bonding is therefore much weaker, 18.6 kcal/mol, than that for ZrH_2. The olefin complexes of niobium and molybdenum follow a similar pattern as the one for zirconium except that there are more valence electrons available and the bonding is therefore never oversaturated as for ZrH_3. Another effect can be noted for these systems for $x = 3$. Even though there is a smaller loss of exchange energy for $x = 3$ than for $x = 2$ the bond strength is smaller for $x = 3$. The reason for this is the rehybridization cost in forming five covalent bonds and also the presence of some direct ligand–ligand repulsion. Similar ligand effects have been noted and studied more in detail previously for the products of the oxidative addition of methane.[12] Oversaturation effects as for $x = 3$ for zirconium are found also for $x = 3$ for yttrium, rhodium, and palladium. In fact, the binding energies in these systems are so weak that they are not considered representative of normal π-bonding and they are therefore not marked in the figure. Also the binding in the rhodium and palladium complexes for $x = 2$ and that in the ruthenium complex for $x = 3$ are rather special cases. In these systems some of the hydrogens form hydrogen molecules which are then weakly molecularly bound to the metal. This situation occurs when the metal has problems forming the necessary number of covalent bonds.

A comment on the geometries of the MH_3 complexes with ethylene can finally be of some general interest. These systems were studied with two different C_s symmetry constraints. In one of these the symmetry plane was taken to go in between the carbon atoms of the olefin and in the other both these carbon atoms are in the symmetry plane. The energy difference between these calculations represents an approximate evaluation of the rotation barrier for the olefin. It turns out that this rotation barrier is quite large for some of the systems. For example, for the molybdenum complex it is 32.8 kcal/mol and for the technetium complex it is 22.8 kcal/mol. The origin of the barrier is a competition for the d_{xy}-orbital of the metal, which should form one of the bonds in the metallacyclic bonding to the olefin. At the top of the rotation barrier, this d_{xy}-orbital should also form a bond to two of the hydrogens and some of these bonds will therefore be weakened at this point.

Since most of the previous studies on the olefin insertion have been done without inclusion of correlation effects, it could be of some interest to make a detailed study of these effects for some systems. The RhH_x transition states were selected for this purpose with the following results (all results include relativistic effects). The insertion barrier for RhH is +32.1 kcal/mol at the SCF level compared to −12.8 kcal/mol at the MCPF level. For RhH_2 the SCF result is much better with a barrier height of −6.4 kcal/mol compared to −0.9 kcal/mol at the MCPF level, but for RhH_3 there is again worse agreement with an SCF result of +18.5 kcal/mol compared to the MCPF result of −3.6 kcal/mol. It is clear that energetic results obtained at the SCF level have to be used with great caution. The relativistic effects are much more stable with effects on the barrier height of 3.8 kcal/mol for RhH, of 1.6 kcal/mol for RhH_2, and of 1.3 kcal/mol for RhH_3.

III. Conclusions

The olefin insertion into a metal–hydrogen bond has been studied for a large number of systems involving second-row transition metals. Repulsion between nonbonding metal electrons and the electrons on the olefin is shown to play a dominant role for the size of the insertion barrier. This effect is best seen for the case without further ligands present and illustrates the usefulness of the present approach where ligand effects are added only at a later stage. Two results that show the importance of this repulsion particularly well can be seen in Figure 2. First, there is a sharp increase in barrier height between niobium and molybdenum both with and without additional hydride ligands present. The explanation for this increase is that niobium can make use of its empty 4d-orbital in an sd-hybridization, which effectively reduces the repulsion toward the olefin. This type of hybridization cannot be used for molybdenum since all nonbonding s- and d-orbitals have the same occupation and the energy is invariant to rotations among these orbitals. Instead, some sp-polarization can be noted for molybdenum, which has important effects for the transition-state geometry (see further in the text). The second point where the consequences of metal–ligand repulsion effects can be clearly seen in Figure 2 is in a comparison for $x = 1$ between rhodium on the one hand and ruthenium and palladium on the other hand. Rhodium has a dramatically lower barrier, which can be explained by the important role played by the s^0-state. For rhodium the s^0-state is low-lying and has the ability to form the covalent d-bond which is required at the transition state. For ruthenium a substantial promotion energy is required to reach the s^0-state, and for palladium the s^0-state has a closed d-shell and can therefore not form any d-bonds. The reason the s^0-state is the dominant state at the transition state must be that repulsive effects play a significant role for the size of the reaction barrier. This state, which is the state with the least repulsion toward ligands, has previously been found to be of key importance for the breaking of both C–H[11,12] and C–C bonds,[13] where rhodium and palladium have the lowest barriers. Another general trend in Figure 2 which can be explained by dominant metal–ligand repulsion effects is the tendency for the atoms to the left in the row to have lower barriers than those to the right. This can be simply explained by the presence of fewer repulsive 4d-electrons for the atoms to the left.

The main effect of adding hydride ligands is a general reduction of the size of the insertion barriers. On the basis of the dominant role of metal–ligand repulsion, this effect is easy to rationalize. The main effect of the hydride ligands is to help in removing some of the repulsive nonbonding electrons from the metal. Since there is no notable reduction of the total charge of the metal, this ligand effect is best described as a charge rearrangement effect. Another trend noted as hydride ligands are added is a reduction of the variation of the barrier heights across the periodic table. Since the main origin of the differences between the metals is the varying degree of repulsion between nonbonding metal electrons and olefin electrons, the removal of some of these metal electrons by the ligand also removes part of the difference between the metals.

It has been demonstrated by the present examples that it is possible to understand the differences between the metals in detail by considering promotion effects, exchange loss effects, sd-hybridization effects, and other metal–ligand repulsion effects. It is of almost equal interest to note the explanations which do not work. One relation which might have been expected is a correlation between metal–hydrogen bond strength and the ease of olefin insertion. However, a general relationship of this type is contradicted by a large number of the presently studied reactions.

For example, TcH has the weakest bond of all the second-row hydrides and yet it has the highest barrier for olefin insertion. There is no relationship between the exothermicity of the insertion reaction and the barrier heights either. In general, there is a very small variation of the exothermicities between the different systems. In contrast, the barrier heights and the binding energies of the π-bonded olefins vary much more. The variations of these latter two energies are finally not correlated either. For example, MoH forms the weakest metal-olefin bond of all the hydrides and has one of the highest barriers for insertion, whereas YH also forms a weak metal-olefin bond but has one of the lowest barriers for insertion.

The present investigation represents an initial study of the important olefin insertion reaction into metal-ligand bonds. Two more studies are underway and will be presented soon. In the first of these studies the olefin insertion into a metal-alkyl bond, which is the main elementary step in the Ziegler-Natta process, will be compared to the present results for the insertion into a metal-hydride bond. In the second future study, the effect on the olefin insertion of adding halide ligands will be investigated.

Appendix A. Computational Details

In the calculations reported in the present paper for the olefin insertion into the second-row transition-metal hydrogen bonds, reasonably large basis sets were used in a generalized contraction scheme[22] and all valence electrons were correlated. Relativistic effects were accounted for using first-order perturbation theory including the mass-velocity and Darwin terms.[23]

For the metal atoms the Huzinaga primitive basis[24] was extended by adding one diffuse d-function, two p-functions in the 5p-region, and three f-functions, yielding a (17s, 13p, 9d, 3f) primitive basis. The core orbitals were totally contracted except for the 4s- and 4p-orbitals which have to be described by at least two functions each to properly reproduce the relativistic effects. The 5s- and 5p-orbitals were described by a double-ζ contraction and the 4d by a triple-ζ contraction. The f-functions were contracted to one function giving a [7s, 6p, 4d, 1f] contracted basis. For carbon the primitive (9s, 5p) basis of Huzinaga[25] was used, contracted according to the generalized contraction scheme to [3s, 2p] and one d-function with the exponent 0.63 was added. For hydrogen the primitive (5s) basis from ref 25 was used, augmented with one p-function with the exponent 0.8 and contracted to [3s, 1p].

In the geometry optimizations at the SCF level described below somewhat smaller basis sets were used. First, for the metal atoms a relativistic ECP according to Hay and Wadt[26] was used. The frozen 4s- and 4p-orbitals are described by a single-ζ contraction and the valence 5s- and 5p-orbitals are described by a double-ζ basis and the 4d-orbital by a triple-ζ basis, including one diffuse function. The rest of the atoms are described by standard double-ζ basis sets.

The correlated calculations were performed using the modified coupled pair functional (MCPF) method,[27] which is a size-consistent, single-reference-state method. The metal 4d and 5s electrons and all electrons on the olefin and hydride ligands except the C 1s electrons were correlated.

All geometries used in the calculations are optimized, either at the SCF level using the GAMESS set of programs[28] or in a few cases at the MCPF (or MP2) level. At the SCF level full optimizations are performed, while in the MCPF optimizations only a few parameters were optimized. It is interesting to note that the most straightforward convergence to reliable geometries was obtained for the transition states of the olefin insertion reaction. The few problems that were encountered in the geometry optimization occurred for some of the π-complexes of the metal atoms to the right, and these are therefore the systems for which the lowest relative accuracy has been obtained in the present study. The origin of this problem is that the binding energy at the SCF level is very small combined with the fact that the binding between the metal and ethylene for ruthenium, rhodium, and palladium is of donation-back-donation type which allows the Hartree-Fock configuration to dissociate correctly into ethylene and a low-lying state of the metal atom. For the metal atoms to the left, on the other hand, the bonding to the olefin is more conventionally covalent and there is therefore no possibility for proper dissociation at the SCF level for these systems. It should further be noted that for some of the SCF optimization symmetry constraints were used, in the first place to reduce computational time in the following MCPF calculation but also to improve convergence of the geometry. When symmetry has been used this has been done for cases where the constraint should have no effect or only a very small effect (less than 1 kcal/mol) on the energy. For the transition-state optimizations, C_s symmetry was used for the MH_3 and some of the MH cases, while no symmetry was used for the MH_2 case. Some of the MH transition states were run both with C_s symmetry and without symmetry, with identical energies as results. For the final alkyl products C_s symmetry was used. For the π-bonded olefin complexes, C_{2v} symmetry was used for the MH_2 case, while C_s symmetry was used for the MH and MH_3 cases.

All results in the tables and figures are from explicit calculations on the given systems except for some of the ethyl complexes. For the naked ethyl systems without hydride ligands, explicit calculations have been made. However, for the ethyl complexes with hydride ligands, the hydride ligand effect has been added from the results of the corresponding methyl systems, published previously.[12] This procedure was tested for the ethyl complexes of yttrium and palladium with one additional hydride ligand and found to be accurate enough for the present purposes.

The results in the tables and in the figures are from the lowest state at each geometrical configuration, which means that energies for different spin and space symmetry are given for the same system at different geometries. This is done mainly because it is the simplest way to display the results in a well-defined way. These results also suggest the most reasonable way the reaction actually proceeds. For systems consisting of only light atoms, reactions normally follow adiabatic surfaces with fixed spin and space symmetry. This is not so for reactions involving transition-metal complexes. For example, Mitchell[29] has shown that in the case of the reaction between a nickel atom and carbonyl, there is near unit probability for jumping between the triplet and the singlet potential energy surfaces at the crossing point. The reason for this is the presence of strong spin-orbit coupling, which should be even stronger for the second-row transition-metal systems studied here.

All the present calculations have been performed on an FX-80 ALLIANT computer and the final energy evaluations were performed using the STOCKHOLM set of programs.[30]

A few words should finally be said about the level of calculation chosen in the present study. As described above the geometries are optimized at the SCF level and the relative energies are

---

[22] (a) Almlöf, J.; Taylor, P. R. *J. Chem. Phys.* **1987**, *86*, 4070. (b) Raffenetti, R. C. *J. Chem. Phys.* **1973**, *58*, 4452.

[23] Martin, R. L. *J. Phys. Chem.* **1983**, *87*, 750. See also: Cowan, R. D.; Griffin, D. C. *J. Opt. Soc. Am.* **1976**, *66*, 1010.

[24] Huzinaga, S. *J. Chem. Phys.* **1977**, *66*, 4245.

[25] Huzinaga, S. *Approximate Atomic Functions*; Department of Chemistry Report, University of Alberta, Edmonton, Alberta, Canada, 1971; Vol. II.

[26] Hay, P. J.; Wadt, W. R. *J. Chem. Phys.* **1985**, *82*, 299.

[27] Chong, D. P.; Langhoff, S. R. *J. Chem. Phys.* **1986**, *84*, 5606.

[28] GAMESS (General Atomic and Molecular Electronic Structure System): Schmidt, M. W.; Baldridge, K. K.; Boatz, J. A.; Jensen, J. H.; Koseki, S.; Gordon, M. S.; Nguyen, K. A.; Windus, T. L.; Elbert, S. T. *OCPE Bull.* **1990**, *10*, 52.

[29] Mitchell, S. A. In *Gas-Phase Metal Reactions*; Fontijn, A., Ed.; Elsevier, Amsterdam, 1992; Chapter 12.

[30] STOCKHOLM is a general purpose quantum chemical set of programs written by Siegbahn, P. E. M.; Blomberg, M. R. A.; Pettersson, L. G. M.; Roos, B. O.; Almlöf, J.

calculated at the MCPF level, i.e. electron correlation effects are included. First, it should be emphasized that the correlation effects on both the reaction energies and the barrier heights are large. In particular, the size of the correlation effects varies strongly across the periodic table so that the diagrams shown in the figures would have appeared very differently if SCF results had been used instead of correlated results. A detailed discussion of correlation effects on metal–ligand binding energies is given in ref 31. The conclusion is that correlation effects have to be included in the calculations to give reliable trends for activation energies and binding energies. Secondly, it can be questioned if the use of SCF-optimized geometries gives reliable results, in particular since the correlation effects are so large. There are several results on systems similar to those studied in the present paper showing that SCF-optimized and MCPF-optimized geometries give very similar relative energies. For example, it was shown in ref 11 for the methane activation reaction that the barrier height for rhodium, the metal with the largest correlation effects in the present context, changed by less than 1 kcal/mol on going from an SCF- to an MCPF-optimized geometry. Also, it is the experience of Bauschlicher and co-workers[32] that if a consistent set of ligand and metal–ligand geometries is used, the binding energies calculated at the MCPF level agree to better than 1 kcal/mol, regardless of whether the equilibrium structures are optimized at the SCF or MCPF level of theory. The origin of this surprising behavior is that in the most interesting region of the potential energy surfaces (including both the transition state and the insertion products) the SCF and the MCPF surfaces are quite parallel. This is seen on the rather small correlation effects on the elimination barriers. For example, for the barrier of ethylene elimination from palladium vinyl hydride[31] the SCF and the MCPF values are identical, and for the corresponding rhodium reaction the correlation effects lower the elimination barrier by only 4 kcal/mol, compared to 56 kcal/mol for the activation barrier. Another reason SCF geometries can be used is that the potential energy surfaces are often rather flat in both the transition-state region and the insertion-product region, so that discrepancies in SCF- and MCPF-optimized structures have very small effects on the relative energies. The conclusion is that the use of SCF-optimized structures gives reliable results for the trends in activation energies and binding energies if correlation effects are included in the energy calculations.

---

(31) Siegbahn, P. E. M.; Blomberg, M. R. A.; Svensson, M. *J. Am. Chem. Soc.* **1993**, *115*, 1952.

(32) Sodupe, M.; Bauschlicher, C. W., Jr.; Langhoff, S. R.; Partridge, H. *J. Phys. Chem.* **1992**, *96*, 2118. Rosi, M.; Bauschlicher, C. W., Jr. *Chem. Phys. Lett.* **1990**, *166*, 189. Bauschlicher, C. W., Jr.; Langhoff, S. R. *J. Phys. Chem.* **1991**, *95*, 2278.